The Relational Harmonics Model

A Geometric Mapping of the Standard Model

Binyamin Tsadik Bair-Mosheh

December 18, 2025

Abstract

We propose the Relational Harmonics Model (RHM) in which spin, electric charge, and color are represented as relational phases organized across three coupled harmonic layers: L_1 **(base persistence and spinor structure)**, L_2 **(charge phase)**, and L_3 **(color phase)**.

Fractional charges ($e/3$, $2e/3$) are mapped to stable phase projections from a regular tetrahedral geometry relative to a leptonic reference, yielding the invariant factor $\cos\theta = -1/3$. Color singlets correspond to vector closure in L_3. Rest mass is interpreted as inter-layer coupling tension, with relativistic kinematics as harmonic consistency constraints.

The RHM is positioned as a structural ontology complementing quantum field theory. Speculative extensions to cosmological radio backgrounds are briefly discussed.

Contents

1 Introduction

The Standard Model of particle physics describes matter fields as irreducible representations of internal gauge groups. While spectacularly successful, this framework typically treats structural features such as fractional charges and color confinement as axiomatic labels attached to fields, rather than as consequences of a deeper internal organization.

The Relational Harmonics Model (RHM) proposes a different starting point: particles are modeled as **localized and persistent harmonic resonances**. In this view, quantum numbers are encoded in, and in some cases constrained by, relational phase differences between the interconnected web of energetic persistence.

The goals of this paper are:

- To define a layered harmonic space (L_1, L_2, L_3) that provides a common geometric setting for spin, charge, and color.
- To show how fractional charges and color singlets can be represented as consequences of specific phase relationships and closure constraints.
- To interpret relativistic kinematics (mass, length contraction) in terms of harmonic stability and conservation of energy for moving localized excitations.
- To distinguish, at the level of ontology, the geometric nature of gravity from the phase-synchronization character of gauge forces.

We will be explicit throughout about which aspects of the construction are postulated (for example, the number of layers and their basic symmetries) and which follow as consequences (for example, the allowed charge projections and color-singlet combinations). The RHM should therefore be read as an early stage proposal for how known quantum numbers might be organized and interpreted within a relational harmonic ontology, rather than as a completed dynamical theory.

2 Layered Harmonic Structure

Within the confines of this model, each localized fermionic excitation is represented as

$$\mathcal{H} = \mathcal{H}_{\mathrm{L1}} \otimes \mathcal{H}_{\mathrm{L2}} \otimes \mathcal{H}_{\mathrm{L3}}, \tag{1}$$

where the three factors track different kinds of internal phase structure that the Standard Model usually encodes as separate quantum numbers. The layers are not additional spatial dimensions, but localized structures allowing for energy to persist in time as spin, electric charge and color, which are collectively measured as rest mass.

We distinguish:

- L_1: The lowest harmonic level, with spinor structure, required for the existence and continuity of higher harmonic structures.
- L_2: a charge phase layer, carrying the structure associated with electric charge and its quantized and fractional values.
- L_3: a color phase layer, carrying the structure associated with color and color-neutral (singlet) combinations.

2.1 L_1: Base Persistence, Spinor Structure, and Stability

We model L_1 as the minimal substrate required for a stable, localized excitation that can accumulate phase over time and participate in interactions. Operationally, L_1 plays the role normally associated with a spinor field in the Standard Model: it carries an internal structure that distinguishes left- and right-handed configurations (ψ_L, ψ_R) and supports fermionic statistics.

In the present ontology we emphasize the left-handed component, in the sense that:

- The L_1 layer provides a "socket" or cavity for a persistent harmonic mode.
- This cavity is intrinsically chiral, so that only certain couplings (for example, weak interactions) can bridge it in a geometrically compatible way.

This picture is meant as a structural interpretation of parity violation: the weak interaction couples preferentially to a specific chiral configuration of the L_1 substrate rather than to a fully symmetric internal space.

We adopt the following working assumptions for L_1:

1. **Internal Frequency:** A localized excitation in L_1 is characterized by a persistent internal angular frequency ω_{L1} in its rest frame. This internal oscillation acts as the excitation's "clock" and defines its temporal identity.
2. **Relational Frame Consistency:** When the excitation is boosted relative to other fermionic cavities, it maintains this internal frequency in its own frame. The familiar relativistic effects (time dilation, length contraction) arise as *relational descriptions* required by other frames to maintain consistency with the invariant ω_{L1}.
3. **The Stability Barrier:** The L_1 cavity cannot be assigned arbitrarily small sizes. We posit that attempting to compress a fermionic cavity to the Planck length L_P would require energy densities comparable to the Planck regime. Consequently, localized fermionic structures are topologically protected against collapse to sub-Planckian sizes under all natural conditions.

Emergence of Velocity Limits From the stability barrier (Assumption 3), a natural limit to Lorentz contraction emerges. For a given excitation with effective wavelength $\lambda_{L_n} \approx hc/E_{L_n}$, the contraction saturates when the characteristic length approaches L_P. This occurs at relative velocities high enough to compress the harmonic structure, but potentially distinct from c.

This suggests a two-stage window: a "soft" velocity limit (set by the saturation of harmonic contraction) and the "hard" limit of c (where cavity size theoretically vanishes). While we do not compute these limits quantitatively here, we note that such effects would only become relevant in extreme gravitational environments.

Note on Neutrinos: Within this framework, a purely L_1 excitation with negligible structure in L_2 and L_3 provides an idealized model for a neutrino-like mode: a persistent chiral cavity with minimal additional phase decoration.

Note on Spin-Statistics and Field Nature In this initial formulation, we utilize complex scalar fields ψ_n to represent the harmonic amplitudes and phase densities of the layered cavities. We emphasize that these scalars are *effective envelope functions* describing the localized energy density and phase relations. We do not claim that the fundamental fermions are bosons; rather, the scalar ψ captures the macroscopic phase coherence of the underlying spinor structure. A rigorous recovery of the Spin-Statistics theorem and the Pauli Exclusion Principle requires upgrading ψ to a spinor-valued

field transforming under the appropriate Clifford algebra. However, the derivation of fractional charges and mass spectral relations depends only on the harmonic phase topology, which is captured adequately by the scalar effective description employed here.

2.2 L_2: Internal Charge Phase Layer

The L_2 layer introduces an internal phase degree of freedom associated with electric charge. In the language of the Standard Model, it is natural to associate this structure with the right-handed spinor component, in the sense that:

- L_1 tracks the base, left-handed persistence mode.
- L_2 contributes an additional phase pattern that, when coupled to L_1, yields the full charged fermion.

An electron, for example, is modeled as a coupled $L_1 \otimes L_2$ system. Its rest energy can be decomposed schematically as

$$E_{\text{electron}} = E(L_1) + E(L_2) + E(L_1/L_2), \tag{2}$$

where $E(L_1)$ and $E(L_2)$ are the intrinsic contributions of the individual harmonic layers ($\hbar\omega_{L_n}$) and $E(L_1/L_2)$ is the coupling energy required to phase-lock the L_2 structure to the L_1 cavity. In this picture, the electron mass is dominated not by a bare "point" mass but by the energetic cost of maintaining a coherent two-layer harmonic configuration.

When related to quarks, the L_2 layer is taken to have a discrete, tripartite phase structure. The charge on each quark comes from a shared L_2 harmonic. A constituent carries three internal phase references which can be arranged in stable patterns corresponding to different effective charge projections. Imposing:

- a finite set of allowed phase differences between the three references,
- a global phase-locking condition that minimizes the coupling energy $E(L_1/L_2)$,

one obtains a discrete set of stable charge assignments. We interpret these as

$$Q \in \left\{ -e, -\frac{2e}{3}, -\frac{e}{3}, 0, \frac{e}{3}, \frac{2e}{3}, e \right\}. \tag{3}$$

In this sense the familiar fractional charges of quarks [2] emerge as geometric consequences of the discrete tripartite structure of L_2, together with a phase-locking constraint that ties L_2 back to the L_1 cavity.
We emphasize that this is a structural representation of known charges in a harmonic paradigm, not a derivation of the fine-structure constant or of dynamical interaction strengths.

2.3 L_3: Color Phase Layer and Hexical Symmetry

The L_3 layer encodes the structure associated with color. Here we postulate a discrete internal symmetry with six allowed phase orientations, corresponding informally to the three "color" directions and their opposites.

$$\phi_{L3}^{(n)} = \frac{n\pi}{3}, \qquad n = 0, 1, 2, 3, 4, 5 \tag{4}$$

A constituent in L_3 is represented by a phase vector $\boldsymbol{c}$ that can occupy one of six allowed orientations in an internal two-dimensional phase space with Z_6 (hexical) symmetry.

A quark-like excitation with all three layers active has an energy budget of the schematic form

$$E_{\text{quark}} = E(L_1) + E(L_2) + E(L_3) + E_{\text{binding}} + E_{\text{closing}}, \tag{5}$$

with

$$E_{\text{binding}} = E(L_1/L_2) + E(L_1/L_3) + E(L_2/L_3) + E(L_1/L_2/L_3). \tag{6}$$

The total rest energy thus reflects not only the intrinsic contributions of each layer but also the combinatorial binding energies between all pairs and the full triplet. The large effective masses associated with strongly interacting quarks are interpreted, in this ontology, as arising from the tension of maintaining a three-layer phase-locked configuration with nontrivial L_3 structure.

Composite objects (such as mesons and baryons) are modeled as bound configurations of multiple L_3 phase vectors. The central constraint is a closure condition

$$\sum_i \boldsymbol{c}_i = 0, \tag{7}$$

which we take as the defining property of color-neutral (singlet) states. In this picture, color confinement is interpreted geometrically: only configurations whose L_3 vectors sum to zero correspond to physically realizable, long-lived excitations.

In this work, we do not attempt to construct the full non-Abelian gage dynamics of QCD from the L_3 structure. Instead, we show how:

- Individual quark-like constituents can be assigned L_3 phase vectors analogous to color charges.
- Color-singlet combinations naturally satisfy the closure condition in the hexical phase space.
- The absence of isolated, non-closed L_3 configurations at low energies can be viewed as a geometric expression of confinement [7, 11].
- Gluons can be viewed as operators on the L3 phase space.

Later sections relate this discrete L_3 phase structure to the familiar color labels of QCD and discuss how gluon-like excitations would appear as transitions between different L_3 configurations.

2.4 Inter-layer Coupling and Weak Reconfiguration

The three layers are not independent. Physical processes correspond to coupled reconfigurations in which the collective harmonic levels adjust in a coordinated way. In particular, weak processes can be viewed, at the level of this ontology, as controlled reconfigurations of the L_2 and L_3 structures on top of a persistent L_1 substrate.

Schematically:

- L_1 tracks which localized excitation persists through the process and how its spinor orientation changes.
- L_2 reconfigures its tripartite phase pattern, changing the effective charge projection (for example, in a neutron-to-proton conversion).
- L_3 adjusts its phase vectors to maintain color closure across initial and final states.

In this picture, a weak interaction event such as beta decay can be interpreted as a finite reconfiguration of the L_2 and L_3 layers, mediated by a bosonic excitation that carries away the necessary mismatch in phase and momentum. The emitted leptons then appear as new L_1-persistent modes with their own L_2 charge phases.

At this stage we do not claim a full reconstruction of the electroweak gauge theory. Rather, we identify a qualitative mechanism by which weak processes can be seen as inter-layer transitions: a redistribution of phase structures across L_1, L_2, and L_3 that preserves overall conservation laws while changing the observable quantum numbers of the participating constituents. Later sections will revisit this interpretation in the context of specific quark-level processes.

3 Electric charge as a harmonic structure in L_2

Having introduced the layered Hilbert space

$$\mathcal{H} = \mathcal{H}_{\mathrm{L1}} \otimes \mathcal{H}_{\mathrm{L2}} \otimes \mathcal{H}_{\mathrm{L3}}, \tag{8}$$

we now make the L_2 structure more explicit. What we construct here is a kinematic model for how the familiar pattern of electric charges

$$Q \in \left\{ -e, -\frac{2e}{3}, -\frac{e}{3}, 0, \frac{e}{3}, \frac{2e}{3}, e \right\} \tag{9}$$

can be represented as a discrete set of internal phase configurations in $\mathcal{H}_{\mathrm{L2}}$, coupled to the L_1 persistence layer.

We do not attempt to derive the value of e or the fine structure constant. Instead, we propose a compact geometric encoding of the *allowed pattern* of charges, in a way that sets up a natural role for coupling energy between L_1 and L_2 as a potentially dominating contribution to rest mass.

3.1 Principle: charge as a harmonic phase relation in L_2

We postulate that L_2 carries an internal harmonic degree of freedom with a characteristic frequency ω_{L_2}. For isolated leptonic states, the relevant structure can be taken to live in an effectively one-dimensional complex phase:

$$\phi_{L_2} \in \mathbb{C}, \qquad \phi_{L_2} = A\, e^{i\phi}, \tag{10}$$

where A is fixed by normalization and ϕ is a phase angle defined *relative to the electron.* By convention we take the electron to set the reference phase $\phi_e = 0$, and then characterize all other leptonic states as phase shifts with respect to this reference:

- The electron corresponds to the reference configuration $\phi = 0$.
- The positron corresponds to a phase-shifted configuration at $\phi = \pi$, representing an inverse wave in the harmonic chamber.

In this restricted leptonic setting, a binary phase structure ($\phi = 0$ vs. $\phi = \pi$) is sufficient to account for the observed pattern of integer charges $\{\pm e\}$. All other signals (e.g., intermediate phases or superpositions) are interpreted as relative phase information measured with respect to this electron reference.

3.2 Forced three-lobe structure in quark arrays

The situation changes when we move from an isolated lepton to a composite excitation such as a baryon. As previously established, an electron or positron can be described, to good approximation, as a single-lobe configuration on its own internal L_2 circle, with a binary phase structure defined by an offset ϕ in the time-dependent harmonic $\psi \propto e^{i(\omega t+\phi)}$. Relative to the electron reference clock, this accounts for the observed leptonic charges $\{-e, +e\}$:

- An electron is a single-lobe configuration aligned with the reference clock: $\psi_e(t) \propto e^{i(\omega t+0)}$.
- A positron is a single-lobe configuration in anti-phase: $\psi_{\bar{e}}(t) \propto e^{i(\omega t+\pi)}$.

By contrast, a baryon contains three distinct quark-like excitations, each with its own local L_2 structure, but all embedded on a common *macro* L_2 orbit. At this macro level, the three quark sectors are arranged at fixed *azimuthal* angular separations of 120° on an effective baryon L_2 circle, while the probing electron defines a phasal reference direction at the center of this circle. The electron's own L_2 phase remains offset by approximately π relative to the baryon's net L_2 mode, but the quarks do not share a single internal oscillation; they occupy three separate phase sectors of a common orbital scaffold. To keep this distinction explicit, we write the baryon's macro configuration as a three-component object

$$\Psi_{\text{baryon}}(t) = \big(\Psi_{q,1}(t), \Psi_{q,2}(t), \Psi_{q,3}(t)\big), \tag{11}$$

where each $\Psi_{q,i}(t)$ denotes the effective quark state in sector i of the baryon's L_2 orbit. Internally, each quark carries its own lobe structure and internal phase dynamics, but on the shared macro circle these three sectors are locked at $(0, 2\pi/3, 4\pi/3)$ in the baryon's co-rotating frame. The key point is that the effective charge attributed to each quark-like constituent is *not* an independently assigned fragment of a shared charge quantum. Instead, it is defined operationally by how often that quark sector presents an electron-like versus positron-like overlap to a probing electron reference. In other words, the measured fractional charge q_i of sector i is a *duty-cycle-weighted* overlap between the quark's internal L_2 activity and the electron's reference oscillator,

$$q_i \;\propto\; \langle \mathrm{Re}[\Psi_{q,i}(t)\, \psi_e^*(t)] \rangle_{\text{cycles}}\,, \tag{12}$$

where the angled brackets denote an average over many internal L_2 cycles and over the relative phase between the baryon macro orbit and the electron clock.

3.2.1 Geometric necessity: the simplex constraint

If the baryon's L_2 phase space were merely a one-dimensional circle, there would be no natural way to distinguish three quark sectors while preserving a single preferred electron-like reference direction. The minimal higher-dimensional structure that accommodates a single electron-like reference direction while treating three quark sectors equivalently is the regular tetrahedron (the 3-simplex). We model the electron as one vertex of this tetrahedron (the "apex") and the three quark sectors as the remaining three vertices (the "base").

Let $\hat{n}_e$ be the unit vector along the electron direction and $\hat{n}_{q,i}$, $i = 1, 2, 3$, the unit vectors toward the three quark sectors. For a centered regular tetrahedron, the simplex closure condition requires

$$\hat{n}_e + \sum_{i=1}^{3} \hat{n}_{q,i} = 0. \tag{13}$$

Taking the dot product with $\hat{n}_e$ gives

$$\hat{n}_e \cdot \hat{n}_e + \sum_{i=1}^{3} \big(\hat{n}_e \cdot \hat{n}_{q,i}\big) = 0. \tag{14}$$

Since $\hat{n}_e \cdot \hat{n}_e = 1$ and, by symmetry, all three electron–quark angles are identical, we write $\hat{n}_e \cdot \hat{n}_{q,i} = \cos\theta$ and obtain

$$1 + 3\cos\theta = 0 \quad \Longrightarrow \quad \cos\theta = -\frac{1}{3}. \tag{15}$$

Thus, the fraction 1/3 is not introduced by hand; it is the invariant projection factor of a regular tetrahedron onto the distinguished electron axis. The corresponding geometric *polar* angle $\theta \approx 109.5^\circ$ fixes the relative tilt of each quark sector with respect to the electron reference direction in the underlying three-dimensional angular space.

When an electron probes a baryon, it does not directly resolve this full tetrahedral configuration. Instead, it samples effective overlaps of its own L_2 mode with the quark sectors as they appear on the baryon's macro L_2 circle (at 0°, 120°, and 240°). The tetrahedral geometry enters as a fixed weighting factor in these overlaps. Schematically, we can write the contribution of a single quark sector to the measured charge as

$$q_{\text{sector}} \;\propto\; Q_e \cos\theta \;=\; Q_e \left(-\frac{1}{3}\right), \tag{16}$$

where Q_e is the electron charge used as the reference scale. Depending on the internal phase alignment of the sector, this projection manifests in one of two stable geometric modes: as a standard single-vertex projection (yielding the down-type magnitude $e/3$), or as a *complementary* double-vertex projection (yielding the up-type magnitude $2e/3$).

In this picture, the hadronic L_2 charge structure is not a sum of three independent "little charges" living on a single shared L_2 wave. Rather, it is the projection of a rigid tetrahedral arrangement of one electron-like axis and three quark sectors onto the one-dimensional timeline of the observer's clock. The observed fractional charges are geometric invariants of this projection, locked in by the fixed relation $\cos\theta = -1/3$ enforced by the simplex constraint, and realized experimentally as stable duty-cycle asymmetries in how each sector overlaps the electron reference.

3.2.2 Geometric Encoding vs. Spatial Orientation

It is crucial to distinguish between external spatial orientation and internal harmonic phase geometry. The tetrahedral structure described here resides in the internal phase space $\mathcal{H}_{L2}$, not in physical $\mathbb{R}^3$. Consequently, the projection angle θ defined by $\cos\theta = -1/3$ does not represent a physical orientation subject to rotational averaging in the laboratory frame. Instead, it represents a fixed *harmonic mixing angle*—a geometric encoding of the coupling efficiency between the quark sector and the electron reference. Just as the Weinberg angle is a fixed parameter of the electroweak interaction rather than a variable spatial direction, the simplex constraint fixes the relative phase-locking efficiency of the constituents, rendering the fractional charge assignments stable and invariant under spatial rotations.

3.3 Mesons as two-lobe shared L_2 structures

Quark–antiquark bound states (mesons) are formed by pairing constituents from the same fundamental geometric alphabet as baryons. Although the meson macro-geometry involves only two

constituents (an effective two-lobe macro scaffold), the phase properties of those lobes are not re-derived from scratch; they are selected from the universal set of stable harmonic modes.

At the level of amplitudes, we represent the mesonic L_2 structure as a time-dependent composite vector

$$\Psi_{\text{meson}}(t) = (\psi_q(t), \psi_{\bar{q}}(t)) \in \mathbb{C}^2, \tag{17}$$

with an overall normalization and a discrete symmetry identifying exchange of the two lobes. The components are oscillating harmonics:

$$\psi_q(t) = A_q e^{i(\omega t + \phi_q)}, \qquad \psi_{\bar{q}}(t) = A_{\bar{q}} e^{i(\omega t + \phi_{\bar{q}})}, \tag{18}$$

with a common net phase Φ_{net} for the meson relative to the electron reference, and individual offsets

$$\phi_q = \Phi_{\text{net}} + \delta_q, \qquad \phi_{\bar{q}} = \Phi_{\text{net}} + \delta_{\bar{q}}. \tag{19}$$

Universality of the Phase Geometry: Crucially, the constituents of a meson are not distinct species from those in a baryon. The constraints derived in the previous section—specifically the **simplex constraint** that fixes the charge projection at magnitudes of $e/3$ and $2e/3$—are properties of the *allowed harmonic modes themselves*.

In a fully relational ontology, there is no background vacuum to impose geometry; rather, geometry emerges from the conditions required for **mutual persistence**. The only stable way for a composite constituent to phase-lock against the fundamental lepton reference is to adopt the phase-tilt of a tetrahedral vertex, with $\cos\theta = -1/3$. This creates a fixed "geometric alphabet" of persistent excitations.

Because the constituents are drawn from this relational set, they retain their simplex-derived charge projections even when bound in pairs. The meson does not revert to a "linear" geometry (which would imply $\pm e/2$ charges) because the internal phase topology of the quark is not a property of its current neighbors, but a property of its fundamental coupling to the electron reference. Each quark-like mode is a vertex of the same underlying simplex relation, and its allowed charge projections are fixed by that harmonic necessity.

The net charge is simply the sum of these fixed projections:

$$Q_{\text{meson}} = q_q + q_{\bar{q}} \in \{0, \pm e\}. \tag{20}$$

We identify two stable classes of interference:

- **Neutral Mesons (Cancellation):** Configurations where the quark and antiquark projections cancel exactly (e.g., $u + \bar{u}$ corresponds to $+2/3 - 2/3 = 0$). The shared L_2 scaffold is present but closed.
- **Charged Mesons (Complementarity):** Configurations where the projections sum to unity (e.g., π^+ composed of $u + \bar{d}$ corresponds to $+2/3 + 1/3 = +1$).

Conceptually, mesons provide the two-lobe analogue of the baryonic three-lobe structure, but both are manifestations of a single macro L_2 phase architecture. In the leptonic sector, a single-lobe configuration suffices (integer charge). In the hadronic sectors, the observed fractional charges emerge because the shared scaffold is populated by constituents geometrically fixed by the tetrahedral simplex constraint, regardless of whether those constituents are bound in pairs or triplets.

3.4 Unified description and the role of L_1–L_2 coupling (zitterbewegung)

Putting these ingredients together, the L_2 layer can be summarized as combining:

1. An internal harmonic with characteristic frequency ω_{L_2} associated with charge degrees of freedom.

2. A phase structure that is effectively one-lobed (binary $0/\pi$) for isolated leptons and three-lobed ($\mathbb{C}^3$) when shared across quark arrays.

3. A phase-locking condition that couples L_2 to the L_1 persistence layer for each localized excitation.

From the standpoint of the Standard Model, this construction does not introduce new charge values or alter known assignments. Its value is structural: it represents all observed charges as different phase placements within a single L_2 harmonic, preparing the ground for a unified account of coupling energies and inter-layer dynamics.

A central feature of the Relational Harmonics Model is that the *mass* of a charged constituent is not attributed solely to an intrinsic self-energy of L_1 or L_2, but to the *tension* required to maintain a stable, phase-locked relationship between them. We write, schematically,

$$E_{\text{charged}} = E(L_1) + E(L_2) + E(L_1/L_2), \tag{21}$$

where $E(L_1/L_2)$ encodes the coupling energy between the L_1 persistence mode and the L_2 charge harmonic. In this model, $E(L_1/L_2)$ plays the role of a zitterbewegung-like term: it reflects an internal jitter or rapid oscillation needed to keep the two layers in a consistent phase relationship.

For light charged fermions such as the electron, we will take $E(L_1/L_2)$ to provide the dominant contribution to the observed rest mass. Heavier constituents, and composite states such as protons, involve additional contributions from L_3 (color) and from collective binding energies, treated in later sections. The present section establishes only the L_2 phase structure and its coupling to L_1; the dynamical implications for kinematics and relativity are developed in Section 5.

4 Color and the Strong Interaction in L_3

Having identified electric charge as an internal harmonic structure of L_2, we now turn to the role of L_3 in encoding color and the strong interaction. In keeping with the relational character of the Relational Harmonics Model (RHM), color is not introduced as an abstract index or label. Instead, it is represented as a discrete phase structure in an internal L_3 harmonic, defined only in relation to other excitations and subject to geometric closure constraints.

We structure this discussion in two parts. First, we present the **Abelian Limit**, a simplified one-oscillator model that provides the geometric intuition for color charges and confinement. Second, we present the **Non-Abelian Extension**, a rigorous three-oscillator description that recovers the full interaction energetics and non-commutative algebra required by Quantum Chromodynamics (QCD).

4.1 The Abelian Limit: Geometric Intuition

We begin with the simplest possible representation of color: a single internal phase oscillator in L_3. While mathematically simpler than full QCD, this geometric picture successfully captures the phenomenology of color neutrality and the "clock-face" nature of gluon exchange.

4.1.1 The one-oscillator model

The L_3 layer is modeled as a harmonic degree of freedom that supports six stable phase configurations, corresponding to three colors and three anti-colors. These are represented as discrete phase angles

$$\phi_{L3}^{(n)} = \frac{n\pi}{3}, \qquad n = 0, 1, 2, 3, 4, 5, \tag{22}$$

equally spaced around a circle in an internal L_3 phase plane. Each allowed phase configuration corresponds to a unit vector $\mathbf{c}_n$. In this picture, the conventional "red, green, blue" labels are simply mnemonic names for three of these discrete L_3 phase vectors.

4.1.2 Geometric confinement

Color-neutral (singlet) states are characterized by geometric closure. For a composite built from constituents indexed by i, with L_3 vectors $\mathbf{c}_i$, we define the net color vector

$$\mathbf{C}_{\text{tot}} = \sum_i \mathbf{c}_i. \tag{23}$$

We then impose color neutrality as the condition $\mathbf{C}_{\text{tot}} = \mathbf{0}$. This immediately reproduces the familiar patterns:

$$\text{baryon:} \quad \mathbf{c}_R + \mathbf{c}_G + \mathbf{c}_B = \mathbf{0}, \tag{24}$$

$$\text{meson:} \quad \mathbf{c}_{\text{color}} + \mathbf{c}_{\text{anti-color}} = \mathbf{0}. \tag{25}$$

Within RHM, confinement is not added as a separate postulate; it is an immediate consequence of the requirement that physically persistent composites must satisfy this closure condition.

4.1.3 Gluons as phase rotations

In this intuitive picture, a gluon exchange is modeled as a discrete rotation of the L_3 phase vectors by a fundamental increment of 60°. A single gluon event corresponds to a quantized 60° phase-rotation on the hex,

$$\mathbf{c}_i \longrightarrow R\left(\pm\tfrac{\pi}{3}\right)\, \mathbf{c}_i, \tag{26}$$

moving a given color phase to its neighboring color/anticolor point. More complicated color rearrangements (such as an effective color-to-color change on the hex) are then represented as algebraic composites of these elementary 60° steps. In all cases, a corresponding, compensating reconfiguration is applied to one or more partner quarks so that the net phase is preserved and color neutrality maintained.

4.2 The Non-Abelian Extension: Full Dynamics

The one-oscillator construction above is minimal. While it reproduces confinement and the basic 60° gluon phase steps, its internal rotation algebra is Abelian (the order of phase rotations does not matter), which deviates from the non-Abelian nature of QCD. To recover the full dynamical consistency of the strong force—including gluons that themselves carry color and non-commuting color generators—we extend the internal color space from one oscillator to three.

4.2.1 The three-oscillator basis and Quark Individuality

In the three-oscillator model, a quark carries a triple of L_3 phases, $\Phi = (\phi_X, \phi_Y, \phi_Z)$. Different colors correspond to different phase "fingerprints" across these three oscillators. A symmetric assignment is:

$$R : (0^\circ, 120^\circ, 240^\circ), \quad G : (120^\circ, 240^\circ, 0^\circ), \quad B : (240^\circ, 0^\circ, 120^\circ), \tag{27}$$

with the corresponding anti-colors obtained by adding 180° to each component.

It is worth emphasizing that in this view, the individuality of the three quarks is not tied to having independent L_3 harmonics. The L_3 level acts as a single multi-sector standing wave. What distinguishes the quarks as separate fermions in the RHM is the presence of three distinct L_1 **cavities**, each providing an independent trapping site that participates in the common internal color modes.

4.2.2 Interaction energetics

We define the harmonic interaction potential between constituents as the sum of cosine phase differences across the three layers:

$$V_{\text{int}} \propto \sum_k \cos(\Delta\phi_k). \tag{28}$$

Calculating this for all pairs yields the Interaction Matrix (Table 1).

Table 1: **Harmonic Interaction Matrix.** Values represent the harmonic cost $\sum \cos \Delta\phi$. Note that like colors (RR) strongly repel (+3.0), while color–anticolor pairs ($R\bar{R}$) form deep attractive wells (-3.0), providing a harmonic basis for meson stability.

	R	**G**	**B**	$\bar{R}$	$\bar{G}$	$\bar{B}$
R	**+3.0**	-1.5	-1.5	**-3.0**	+1.5	+1.5
G	-1.5	**+3.0**	-1.5	+1.5	**-3.0**	+1.5
B	-1.5	-1.5	**+3.0**	+1.5	+1.5	**-3.0**

4.2.3 Explicit non-Abelian commutators

While the single-oscillator rotation picture above provides the geometric intuition, the full dynamical consistency of QCD requires that color operations be *non-commutative* (non-Abelian) so that gluons themselves carry and exchange color.

To make this structure explicit, we pass to the abstract color basis (R, G, B) corresponding to distinct phase fingerprints on the three L_3 oscillators. In this basis, we identify the operator $T_{R\bar{G}}$ that converts a Green fingerprint into a Red fingerprint. It is important to note that in the geometric hex model, R and G are separated by 120°. Therefore, this standard QCD operator corresponds geometrically to a composite of two elementary 60° steps (or a net 120° rotation).

The operator is represented as:

$$T_{R\bar{G}} = |R\rangle\langle G| = \begin{pmatrix} 0 & 1 & 0 \\ 0 & 0 & 0 \\ 0 & 0 & 0 \end{pmatrix}, \tag{29}$$

with its conjugate $T_{G\bar{R}} = |G\rangle\langle R|$ implementing the reverse change:

$$T_{G\bar{R}} = \begin{pmatrix} 0 & 0 & 0 \\ 1 & 0 & 0 \\ 0 & 0 & 0 \end{pmatrix}. \tag{30}$$

A simple diagonal color operator that distinguishes Red from Green is

$$H_{RG} = |R\rangle\langle R| - |G\rangle\langle G| = \begin{pmatrix} 1 & 0 & 0 \\ 0 & -1 & 0 \\ 0 & 0 & 0 \end{pmatrix}. \tag{31}$$

Evaluating the commutators yields

$$[H_{RG}, T_{R\bar{G}}] = H_{RG}T_{R\bar{G}} - T_{R\bar{G}}H_{RG} = 2\,T_{R\bar{G}}, \tag{32}$$

and

$$[H_{RG}, T_{G\bar{R}}] = H_{RG}T_{G\bar{R}} - T_{G\bar{R}}H_{RG} = -2\,T_{G\bar{R}}, \tag{33}$$

which are manifestly non-zero. This reproduces the structural pattern of the SU(3) Lie algebra, where diagonal generators do not commute with off-diagonal color-changing generators.

Thus, the RHM framework bridges the two views: the *intuitive* picture of discrete 60° phase rotations on the hex (the fine structure), and the *formal* non-Abelian matrix algebra acting on the (R, G, B) basis (the effective theory). In this way, the explicit commutator relations show that the color sector of RHM is genuinely non-Abelian in the same structural sense as QCD, while retaining a concrete geometric foundation.

5 Mapping to Kinematics and Relativity

In the Relational Harmonics Model, kinematical quantities such as velocity, momentum, and relativistic invariants are understood as geometric features of underlying harmonic structures rather than as primitive inputs defined on a pre-existing spacetime background. Crucially, time itself is not taken as fundamental: it emerges only when bosonic excitations are trapped into localized, persistent fermionic cavities and compared against one another.

A freely propagating boson, whose wave is not tightly tied to a particular spatial path, does not carry a localized internal cycle that can serve as an operational clock. In the idealized limit of unbound propagation, its effective passage through space can be advanced or delayed without selecting a unique, localized temporal parameter. In this regime, it is meaningless to speak of an isolated boson as "experiencing" proper time in the same way a massive particle does.

A fermion, by contrast, is precisely such a trapped configuration: bosonic modes are locked into a stable, localized cavity and forced into a persistent, cyclic pattern. The internal harmonics of this cavity then furnish a well-defined internal period. In conventional language, this internal cycle plays the role of the particle's proper time. A single fermionic cavity, however, does not register any relativistic effect from its own perspective; its internal oscillation simply repeats, and there is no operational notion of "time dilation" or "length contraction" available to it in isolation.

Relativistic structure enters only when two or more such fermionic cavities are present and their internal cycles are compared. Each cavity carries its own persistent harmonic structure, with characteristic binding frequencies and phase relations. When one cavity is used as a relational frame to describe another, the requirement that rest mass and energy be conserved imposes non-trivial constraints: the internal frequencies and phases assigned to a given cavity must match, up

to a consistent reparametrization, in every fermionic frame that measures them. From this point of view, Lorentz invariance appears as a relational matching rule between fermionic clocks, rather than as a modification of any individual cavity's intrinsic experience.

This section sketches how the familiar apparatus of special relativity can be recovered from the behavior of persistent fermionic cavities, their internal modes, and the consistency constraints imposed when different cavities compare their emergent clocks.

5.1 The constant c as a normalization boundary

Within RHM, the speed of light c appears as a fundamental, invariant **normalization boundary** between two regimes:

- Internal harmonic variables, such as momentum p, can take arbitrarily large values in principle, reflecting how strongly a localized cavity is deformed or excited.
- Observable relative speeds v between fermionic structures are confined to the finite range $v \in [0, c)$.

The role of c is to map the unbounded internal momentum scale $p \in [0, \infty)$ onto the bounded kinematical scale of relative velocity. In this sense, infinite relative momentum corresponds to the asymptotic speed limit $v \to c$, and c acts as an emergent normalization boundary rather than a freely chosen unit conversion.

5.2 Harmonic contraction and the origin of Lorentz invariance

In the RHM picture, relativistic kinematics are not axioms of an independent spacetime arena, but geometric responses of harmonic cavities to motion relative to other persistent structures. The key assumption is that the internal modes which define a fermion evolve with respect to the fermion's own proper time τ, with a characteristic binding frequency ω_0 that is invariant under motion.

Consider a fermionic cavity whose internal L_1–L_2 structure defines a rest mass through some proper-time binding frequency ω_0. In the cavity's own rest frame this appears as a stationary, cyclic pattern of internal phases

$$\psi(\tau) \sim e^{-i\omega_0 \tau},$$

with a time-independent spatial profile. From that perspective there is no relativistic effect: the internal cycle simply repeats with frequency ω_0 in its own proper time. In RHM, the rest energy and rest mass of the fermion are just re-expressions of this intrinsic cycle,

$$E_0 = \hbar\omega_0, \qquad m_0 = E_0/c^2.$$

When another fermionic cavity is used as a relational observer, the same internal cycle must be described in terms of that observer's coordinate time t and space x. For an observer in relative motion with speed v, the internal oscillation is seen as evolving in t with the usual time-dilated rate

$$\omega_{\text{obs}} = \frac{\omega_0}{\gamma}, \qquad \gamma = \frac{1}{\sqrt{1 - v^2/c^2}}.$$

What changes between frames is not the proper-time frequency itself, but the way proper time is sliced into coordinate time and space. All observers must ultimately recover the same underlying binding frequency ω_0, and thus the same rest-mass assignment, when they infer the intrinsic cycle of a given cavity.

Within RHM, the geometric response of the cavity to motion must accommodate this relational description. As the cavity is boosted, its spatial extent along the direction of motion must contract in such a way that the full pattern of internal phases remains compatible with a single invariant proper-time evolution when seen from any other fermionic frame. The familiar Lorentz contraction of external spatial lengths is reinterpreted as the adjustment required so that the internal proper-time cycle of the moving cavity can be consistently embedded into the emergent time coordinate of another cavity without violating energy conservation or rest-mass assignments.

From this perspective:

- **Mechanism:** Time dilation describes how one fermionic cavity must see another's internal clock as slowed when expressed in its own emergent time coordinate. Lorentz contraction and the relativity of simultaneity then fix how the spatial profile of the moving cavity is deformed so that the complete internal phase pattern remains consistent with the same invariant proper-time cycle. The result is the usual Lorentz geometry in external spacetime.
- **Momentum as geometric constraint:** Momentum is not a primitive cause of geometric shortening. Rather, what we call *momentum* measures how strongly the cavity has been reconfigured in the direction of motion in order to preserve its internal proper-time harmonic while relating it to an external coordinate frame. The standard relation between momentum and velocity reflects a specific mapping between this geometric deformation and relative speed.

On this account, Lorentz invariance arises because the laws governing the internal harmonics—their proper-time frequencies and phase relations—are the same for all fermionic cavities, and the allowed deformations under relative motion are uniquely fixed by the requirement that all observers recover the same intrinsic binding frequency (and thus the same rest mass) when they compare cycles.

5.3 Mass as coupling tension and Zitterbewegung

In the RHM, the rest mass of a fermion is dominated not by some static substance but by a dynamic **coupling tension** between harmonic layers. For the electron, it may be that the overwhelming contribution to the rest mass m_e comes from the binding energy associated with chiral mixing:

- The L_1 layer encodes persistence and localization.
- The L_2 layer encodes charge and its phase relations.
- A topological phase-lock between L_1 and L_2 must be maintained for the electron to exist as a stable, persistent cavity.

The energetic cost of maintaining this phase-lock can be identified with the rest mass energy $m_e c^2$. Historically, the necessity of a non-electric stress to stabilize a charged particle against its own repulsion was identified by Poincaré [9]. In the RHM, this "Poincaré stress" is reinterpreted as the harmonic tension required to keep the two layers in a consistent phase relationship. The rapid internal oscillation sometimes associated with *zitterbewegung* in relativistic wave equations is reinterpreted here as the internal chiral mixing

5.4 The weak interaction and harmonic reconfiguration

Within this framework, the weak interaction is naturally modeled as a mechanism for **harmonic reconfiguration** of layered structures, rather than as a purely abstract change of internal quantum numbers.

In a process such as electron capture,

$$p + e^- \to n + \nu_e,$$

the proton's internal quark structure is reconfigured into that of a neutron, while an electron is removed from the atomic environment. In RHM terms:

- The electron's L_2 (charge) layer can be absorbed into the composite quark structure as part of a new harmonic configuration consistent with the neutron.
- The electron's L_1 persistence layer is not fully required in the final bound state and is instead ejected as a separate, weakly interacting structure: the neutrino.

The neutrino is thus interpreted as **harmonic debris**—a residual L_1-dominated structure that carries away excess persistence and phase information that cannot be absorbed into the new hadronic configuration. Its extremely small mass and weak interactions follow from the fact that it retains only a minimal harmonic coupling to the richer L_2 and L_3 structures present in charged leptons and hadrons.

From this point of view, weak processes are those in which the internal harmonic layering of particles is rearranged, with neutrinos acting as the carriers of leftover persistence that must be expelled to satisfy the closure and binding constraints of the final state.

6 Forces and Interactions

In the Relational Harmonics Model, forces are not introduced as independent fields acting within a pre-given spacetime. Instead, they arise as dynamical adjustments of the layered harmonic relations among persistent fermionic structures. What are usually called "gauge fields" appear as collective modes that track and enforce the internal phase constraints of the L_2 and L_3 harmonics as particles move and interact.

6.1 Gauge forces as harmonic bookkeeping

The L_2 and L_3 modes carry phases whose configurations encode electric charge and color. As fermionic cavities move relative to each other, or exchange internal excitations, these phases must be updated in a way that preserves the closure conditions defining each stable structure. From the RHM perspective:

- **Gauge bosons** are not substances in a background vacuum, but quantized adjustments in the relational phases of the underlying harmonics.
- The familiar gauge symmetries (U(1), SU(2), SU(3)) organize the allowed patterns of these phase adjustments that leave the local harmonic "rules" invariant.

The standard gauge fields thus serve as bookkeeping devices for how the relational geometry of L_2 and L_3 must change when charges and colors are redistributed, subject to energy conservation and the discrete spectrum of allowed harmonic transitions.

Note on Gauge Fields as Phase Bookkeeping In the Standard Model, gauge invariance dictates the form of interactions via the covariant derivative D_μ. The RHM offers a geometric ontology for *why* these specific symmetries exist. We posit that the gauge fields (photons, gluons) act as the

necessary "bookkeeping" agents that track phase discrepancies between moving harmonic cavities. While this paper focuses on the geometric origin of these phase constraints (the "structural layer"), we anticipate that the full dynamical evolution of these phase adjustments matches the Yang-Mills action in the continuum limit. We do not here derive the Maxwell or QCD Lagrangians from first principles, but rather identify the specific harmonic closure conditions that the standard gauge fields function to preserve.

6.2 Electromagnetism as L_1–L_2 phase tracking

In the RHM, electromagnetic behavior does not live in an independent field substance, but in the way fermionic cavities coordinate their internal L_1 and L_2 phases. Electric charge is encoded in the configuration and orientation of the L_2 harmonic, while the particle's proper-time evolution and spin content are set by its L_1 cycle. A charged fermionic cavity carries a non-trivial L_2 phase pattern, locked to a particular L_1 phase/handedness structure, and this combined L_1–L_2 pattern cannot be locally erased without violating the closure conditions that define the particle.

An electron and a positron share the same proper-time binding frequency at L_1, but have oppositely oriented L_2 configurations: they carry conjugate L_2 charge phases, and their L_1 phases are related by a conjugation that makes them opposites in the sector that couples to neutrino-like modes. As a result, their combined L_1–L_2 pattern is capable of complete recombination when they overlap, with no leftover handedness that would have to be exported into a neutrino cavity.

As charged fermions move, the L_2 phases that encode their charge, and their locking to the underlying L_1 cycles, must be kept consistent along any path in the relational network. What appears in conventional language as a U(1) electromagnetic field is, in the RHM picture, just the minimal relational structure required to track and reconcile these coupled L_1–L_2 phase changes. Photons then correspond to discrete, propagating adjustments of this phase bookkeeping, with their concrete form fixed by how the L_1–L_2 pattern recombines and by the Maxwell equations, subject to the normalization boundary set by c.

More explicitly:

- **Photons** are quanta of L_2 phase reconfiguration, locked consistently to the L_1 proper-time cycles of the interacting fermionic cavities. Their frequencies are set by the differences in L_1 binding energy between initial and final configurations, and their polarizations encode the changes in angular momentum implied by the underlying L_1 spin structure.

- The Maxwell equations summarize how time-dependent L_2 reconfigurations, sourced by changing charge and current patterns in the fermionic cavities, evolve into well-defined electromagnetic wave patterns. In RHM terms, they enforce a unique mapping from a given L_1–driven recombination history of the L_2 pattern to the allowed outgoing electromagnetic harmonics.

In this picture, the electromagnetic interaction is the tendency of the system to move toward L_1–L_2 configurations that lower the overall harmonic energy (for example, by separating like charges and bringing opposite charges together), with the photon spectrum reflecting the discrete energy differences between allowed L_1–L_2 configurations.

Electron–positron annihilation is best understood in this framework as a recombination event rather than a disappearance. An electron and a positron are fermionic cavities with opposite L_2 charge phases and opposite contributions in the L_1 sector that couples to neutrino-like modes, so that their combined L_1–L_2 pattern is harmonically self-contained. When they overlap, their localized charge and current patterns do not simply vanish; instead, their L_1 cycles and L_2 phases undergo a rapid, highly constrained recombination. This time-dependent recombination pattern of

the L_1–driven L_2 configuration is precisely what acts as the source for the Maxwell equations on the relational network.

For a nearly at-rest e^+e^- pair, the unique Maxwell-compatible recombination pattern is a pair of counter-propagating electromagnetic wave packets with energies 0.511 MeV each: two gamma photons whose frequencies and polarizations encode the total energy and angular momentum originally carried by the electron and positron. No neutrino is required, because the relevant L_1 phase components that would otherwise have to be exported into a neutrino cavity are already canceled in the recombined L_1–L_2 pattern of the pair. In this way, "annihilation" is a complete recombination event at the level of localized charged L_1–L_2 cavities, with their conserved energy and spin preserved and re-expressed as a specific electromagnetic oscillation pattern determined by the Maxwell equations, rather than as excitations of an independent field substance.

6.3 Strong interaction as L_3 closure dynamics

Color charge resides in the L_3 harmonic as a three-component phase structure subject to a closure constraint: color-neutral states minimize a closure energy functional by arranging their L_3 phase vectors so that the net color vector vanishes. Quarks correspond to localized cavities with nontrivial L_3 orientation; hadrons are composite structures in which these orientations close.

Gluons appear as L3 phase-rotation quanta that actively reconfigure the color orientations of quarks while preserving color closure at the network level:

- In standard QCD there are eight gluons. In the RHM picture, all of them are L_3 phase-rotation quanta built from the same discrete internal step, but they differ by *how* they act on the three color directions.
- Six gluons correspond to 60° rotations on the L_3 color hexagon, each starting from a different color or anticolor and rotating toward a neighboring direction; these are the off-diagonal modes that effectively convert one color into another.
- The remaining two gluons are diagonal L_3 modes constructed from 180° phase flips distributed across the three color directions, encoding two independent contrasts among R, G, and B.

Together, these six 60° rotations and two 180°-based contrast modes span the same eight-dimensional space of color rotations as the eight gluons of $\mathrm{SU}(3)_c$, but are represented here as discrete geometric reconfigurations of the L_3 harmonic. Confinement is the statement that isolated, non-closed L_3 configurations carry a rapidly increasing closure energy, making them inaccessible as asymptotic states.

6.4 Weak interaction as harmonic reconfiguration

In the weak sector, the RHM emphasizes that flavor change is accompanied by a partial reconfiguration of the internal harmonic layers. Processes such as beta decay are modeled as:

- A redistribution of L_2 and L_3 structure among the participating fermionic cavities, mediated by massive gauge bosons that represent large, localized adjustments to the internal harmonic phases.
- The appearance of neutrinos as "harmonic debris": minimal L_1–L_2 structures that carry away whatever residual phase and energy cannot be consistently integrated into the final bound state.

The large effective masses of the $W^{\pm}$ and Z^0 bosons reflect the high energetic cost of such concentrated, multi-layer reconfigurations of the harmonic structure, and the short range of the weak interaction follows from the fact that these configurations are only barely compatible with the closure constraints that define stable cavities.

6.5 Gravitational effects as emergent geometric distortion

Because the RHM ontology is fully relational, there is no fixed background spacetime in which interactions occur. Instead, the metric properties of spacetime are understood as emerging from the collective relational structure of many persistent fermions and their harmonic couplings.

Motivated by the empirical success of General Relativity, we may hypothesize that gravitational phenomena reflect changes in the effective harmonic environment induced by large aggregations of harmonic energy:

- The total harmonic energy carried in L_1, L_2, L_3, and binding terms defines the size and shape of the "harmonic cavities" that underwrite persistence.
- Variations in this total density lead to **geometric distortion** (curvature) of the emergent relational geometry, biasing the geodesics of all propagating quanta without requiring a mediating particle in a pre-existing vacuum[14].

At the scale of individual fermions such effects are negligible in the same way that a grain of sand does not represent the curvature of the earth; gravity becomes meaningful only as an emergent, coarse-grained characterization of the collective harmonic configuration of many particles.

6.6 Mass Generation and the Higgs as a Collective Mode

In the Standard Model, the Higgs field is introduced as a fundamental scalar whose vacuum expectation value generates masses for leptons and quarks via Yukawa couplings. The RHM framework recovers this phenomenology while shifting the ontology: rest mass arises from the **geometric tension** required to maintain phase-locking between harmonic layers (e.g., $E_{L1/L2}$).

In this picture, the "Higgs Field" is the effective description of the background tension of the coupled $L_1 \otimes L_2 \otimes L_3$ harmonic network. Consequently, the 125 GeV Higgs Boson observed at the LHC[1, 12] is interpreted not as a fundamental elementary particle but as the quantized **breathing mode** (phonon) of this relational lattice.

This interpretation naturally reproduces the Standard Model coupling pattern, $g_{Hff} \propto m_f$. Since the rest mass m_f of a fermion is literally the measure of the stored harmonic tension in its configuration, the coupling of the lattice's breathing mode to that fermion is necessarily proportional to the tension already present. Thus, the RHM framework accommodates the observation of Higgs decays to heavy leptons ($H \to \tau^+\tau^-, \mu^+\mu^-$) as the dissipation of lattice excitations into the specific harmonic tension modes of the lepton cavities.

6.7 An Illustrative Model: The Scalar Lagrangian

The Lagrangian presented in this section is intended as a minimal *effective field theory* that illustrates the mechanism of harmonic phase-locking in the Relational Harmonics Model. For clarity, we utilize three complex scalar order parameters ψ_j which, in the absence of inter-layer coupling, would each enjoy their own global $U(1)$ phase symmetry (a total $U(1)^3$ symmetry). The RHM closure terms explicitly reduce this to a single diagonal $U(1)$, reflecting the fact that only the collective overall phase is physically redundant once geometric closure is imposed.

We introduce the fields:

$$\psi_1(x), \quad \psi_2(x), \quad \psi_3(x), \tag{34}$$

representing the coarse-grained harmonic amplitudes and phases on the L_1, L_2, and L_3 layers, respectively. Locally, each field may be written in polar form as $\psi_j = A_j e^{i\phi_j}$.

A minimal Lorentz-invariant RHM Lagrangian density takes the form:

$$\mathcal{L}_{\text{RHM}} = \mathcal{L}_{\text{kinetic}} - V_{\text{harmonic}} - V_{\text{closure}}\,. \tag{35}$$

The kinetic sector is taken to be canonical:

$$\mathcal{L}_{\text{kinetic}} = \sum_{j=1}^{3} \partial_\mu \psi_j^* \, \partial^\mu \psi_j, \tag{36}$$

and the intrinsic "harmonic" cavity potentials are:

$$V_{\text{harmonic}} = \sum_{j=1}^{3} \left(m_j^2 \, |\psi_j|^2 + \lambda_j \, |\psi_j|^4 \right) + \sum_{j<k} \lambda_{jk} \, |\psi_j|^2 |\psi_k|^2. \tag{37}$$

Here m_j^2 and λ_j encode the intrinsic curvature and self-interaction of each harmonic cavity, while the symmetric λ_{jk} terms allow for density mixing even in the absence of phase-locking.

The characteristic RHM structure is encoded in the closure potential, which energetically enforces geometric relations between the phases:

$$V_{\text{closure}} = -\kappa \left(\psi_1^2 \, \psi_2^* \psi_3^* + \psi_1^{*2} \, \psi_2 \psi_3 \right) + \sum_{j<k} \eta_{jk} \left(|\psi_j|^2 - |\psi_k|^2 \right)^2. \tag{38}$$

The tri-linear term proportional to κ couples the phases of all three layers. Writing $\psi_j = A_j e^{i\phi_j}$, this contribution can be expressed as:

$$V_\kappa = -2\kappa \, A_1^2 A_2 A_3 \, \cos(2\phi_1 - \phi_2 - \phi_3)\,, \tag{39}$$

which is minimized when the resonance condition

$$2\phi_1 - \phi_2 - \phi_3 \approx 0 \pmod{2\pi} \tag{40}$$

is satisfied. This term therefore implements the geometric phase-locking constraint between L_1 and the composite L_2–L_3 structure. The remaining η_{jk} terms are "density-locking" potentials that drive the system toward equal harmonic intensities $|\psi_j|^2 \simeq |\psi_k|^2$.

Mass Generation from Closure. To see how closure generates mass gaps, we expand around a spatially uniform, phase-locked vacuum. For illustrative purposes, we assume a symmetric configuration

$$\psi_j(x) = v \, e^{i\bar{\phi}_j} + \delta\psi_j(x), \tag{41}$$

where the background phases satisfy the resonance condition (40) and v is a common amplitude.

Expanding the potential schematically to quadratic order in the fluctuations, one finds:

- One exactly **massless phase mode**, corresponding to the unbroken diagonal $U(1)$ (overall phase rotation);

- Two **massive phase combinations**, whose squared masses are proportional to κv^2, reflecting the energetic cost of violating the resonance condition;
- Three **massive amplitude modes**, with masses set by the m_j^2, λ_{jk} and η_{jk} parameters.

A convenient way to make this structure explicit is to decompose the three phases into one overall phase and two relative combinations, e.g.:

$$\theta_0 = \frac{1}{3}(\phi_1 + \phi_2 + \phi_3), \tag{42}$$

$$\theta_1 = \phi_1 - \phi_2, \tag{43}$$

$$\theta_2 = \phi_1 - \phi_3. \tag{44}$$

The closure term V_κ depends only on the relative phases $\theta_{1,2}$ through the combination $2\phi_1 - \phi_2 - \phi_3$, while the overall phase θ_0 drops out. At quadratic order around the minimum, the potential is independent of θ_0 (yielding the massless Goldstone mode) but contains harmonic terms for $\theta_{1,2}$ with curvature set by κv^2, corresponding to the two massive phase modes discussed above.

In this way, the RHM notion of "geometric closure" is realized as a standard symmetry-breaking mechanism: the inter-layer coupling terms lift all but one phase direction, leaving a single global $U(1)$ Goldstone mode and a discrete set of stable, gapped cavity excitations.

By power counting, the Lagrangian (38) involves only operators of mass dimension four and is therefore strictly renormalizable [8]. While this scalar model does not capture the spin-statistics of the fermionic L_1 layer, it serves as a Ginzburg–Landau–type effective theory for the collective cavity amplitude. Our goal here is not to reconstruct the full electroweak sector, but to isolate and make explicit the phase-locking and closure mechanism in the simplest possible setting. In a more complete realization, the scalar order parameters ψ_j would be replaced by fields carrying the appropriate $SU(2) \times U(1)$ electroweak charges, and the closure term would be promoted to a gauge-invariant interaction in that larger internal space.

7 Discussion

7.1 Scope: Structural Ontology vs. Scattering Dynamics

The RHM is presented here as a structural ontology—a map of *what* the elementary particles are in terms of harmonic geometry—rather than a dynamical calculus for scattering amplitudes. We do not explicitly compute cross-sections (e.g., $e^+e^- \to \mu^+\mu^-$) or derive Feynman rules in this work. We assume that, to leading order, the perturbative scattering behavior of these harmonic cavities is effectively described by Standard Model QFT. The utility of the RHM lies in its ability to explain the origin of the quantum numbers (charge, color) and to predict macroscopic spectral features (the Kinematic Horizon) that are inaccessible to perturbative QFT.

7.2 Limitations and Open Problems

The Relational Harmonics Model, as presented here, is a structural framework rather than a complete dynamical theory. Key limitations include:

1. **Absence of Scattering Amplitudes:** We do not currently derive Feynman rules or calculate cross-sections (e.g., $e^+e^- \to \mu^+\mu^-$). Standard Model perturbative dynamics are assumed to hold to leading order.

2. **Gauge Dynamics:** The Lagrangian formulation (Sec. 6.8) utilizes Abelian scalars to demonstrate phase locking; a full embedding into the non-Abelian Standard Model gauge group is left for future work.

3. **Horizon Coupling Mechanism:** The conversion of horizon geometric stress into electromagnetic radiation is treated phenomenologically. A rigorous derivation of this coupling via vacuum polarization loops remains an open problem.

Despite these limitations, the model provides a unique, falsifiable phenomenology regarding the geometric origin of quantum numbers and the spectral structure of the cosmic radio background.

7.3 Emergent Time: The Buffer Effect

A central insight of the RHM is that Fermions act as **Time Buffers**. When a fermion absorbs a boson (propagating energy), the energy is captured into the localized harmonic structure. This allows the instantaneous and timeless boson to "sit still" and accumulate phase cycles within the fermion before being re-emitted. This delay—the conversion of propagation into persistence—is the physical origin of the flow of time.

7.4 Entropy and coarse-grained energy density

In the RHM, the fundamental descriptors of a configuration are the local harmonic amplitudes and phases in the L_1, L_2, and L_3 layers, together with the coupling and closure constraints they must satisfy. These microscopic variables determine local energy densities, charge assignments, and fluxes, but they carry far more information than is typically accessible to a coarse-grained observer.

From this perspective, entropy is not a primitive quantity added on top of the dynamics, but a derived measure of how many distinct L_1–L_2–L_3 phase configurations realize the same macroscopic profile of energy and charge. For a given coarse-grained description of the relational network (specified, for example, by averaged energy densities, charge densities, and fluxes in each region), the entropy is defined as the logarithm of the number of micro-harmonic assignments of amplitudes and phases that satisfy all RHM closure constraints while reproducing that coarse profile.

In this sense, entropy in the RHM is directly tied to energy density, but not reducible to it. A highly localized, sharply organized configuration of L_1–L_2–L_3 phases (such as a few well-defined fermionic cavities with clean phase-locked relations) has low entropy, because only a small set of micro-harmonic patterns is compatible with its macroscopic description. As energy spreads out and becomes distributed over many weakly correlated degrees of freedom, the number of compatible L_1–L_2–L_3 configurations grows rapidly, and the entropy increases, even if the coarse-grained energy density changes only modestly.

The directionality usually attributed to the "arrow of time" can then be rephrased in RHM terms: typical evolutions of the relational network carry initially fine-tuned L_1–L_2–L_3 phase patterns into states where energy is more evenly distributed and detailed phase relationships are more scrambled. The underlying harmonic equations remain locally reversible, but almost all initial conditions compatible with a given low-entropy macrostate evolve into macrostates that can be realized by far more micro-harmonic configurations. Entropy growth is thus a statement about the combinatorics of allowed RHM microstates, not a fundamental asymmetry in the local laws.

This picture dovetails with emergent time, which corresponds, at the micro-harmonic level, to the gradual redistribution of L_1 cycle tension and L_2/L_3 phase structure across many relational links. When viewed through a coarse-grained description that only tracks energy densities and conserved charges, this redistribution appears as a monotonic increase of entropy. In RHM language,

the "second law" states that, given the same coarse macroscopic constraints, almost all accessible L_1–L_2–L_3 configurations are ones in which harmonic energy is more widely spread and phase correlations are less structured.

7.5 Prediction: The Kinematic Horizon Spectrum

The RHM interprets the observable universe as a **Kinematic Horizon** where the recession velocity of the harmonic network approaches light speed ($v \to c$). We derive the observational signature of this horizon based on the rest mass of the particles reaching it.

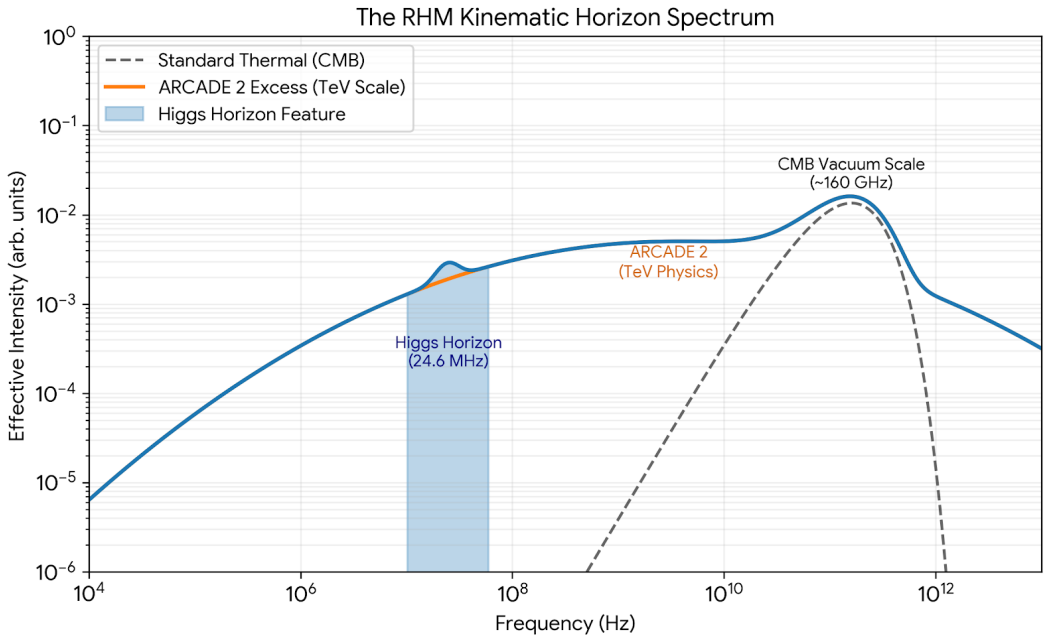

Figure 1: **The RHM Spectral Map.** A log-log plot illustrating the kinematic horizon signatures. The black dashed line represents the standard thermal background (CMB). The orange region highlights the ARCADE 2 excess (interpreted here as TeV-scale physics). The blue peak at ~ 25 MHz is the predicted "Higgs Horizon Feature."

7.5.1 Derivation of the Horizon Frequency

It is essential to distinguish between the intrinsic Compton frequency of a particle and its observed signature at the kinematic horizon. In the particle's rest frame, the standard quantum relation $E = hf_s$ holds. However, radiation emitted from the harmonic network at the kinematic horizon is subject to extreme relativistic effects.

In the ultra-relativistic limit ($\gamma \gg 1$), the observed frequency f_{obs} of a source receding at velocity v is related to the source frequency f_s by the relativistic Doppler factor:

$$f_{\text{obs}} \approx \frac{f_s}{2\gamma}. \tag{45}$$

The RHM imposes a stability barrier: the Lorentz contraction of the harmonic cavity saturates when the contracted wavelength approaches the Planck length L_P. This defines a maximum Lorentz

factor for the cavity:

$$\gamma_{\max} \approx \frac{\lambda_C}{L_P} = \frac{h}{mcL_P}. \tag{46}$$

Substituting $f_s = mc^2/h$ and $\gamma_{\max}$ into the Doppler equation yields:

$$f_{\text{obs}} \approx \frac{mc^2/h}{2(h/mcL_P)} = \frac{m^2c^3L_P}{2h^2}. \tag{47}$$

Mechanism of Emission: We treat the predicted background signals as *effective electromagnetic emissivities* of the horizon. We do not claim that neutral fields (like the Higgs) oscillate coherently at radio frequencies. Rather, the mass scale m defines the dominant tension of a harmonic sector. When this sector saturates at the horizon, geometric stress couples to the charged sector (vacuum polarization), inducing broadband electromagnetic noise centered at f_{obs}.

7.5.2 Spectral Map and New Predictions

We apply this formula to known Standard Model masses and observed background anomalies. Note that because $f_{\text{obs}} \propto m^2$, small changes in mass scale correspond to significant shifts in observed frequency.

Source Mass (m)	**Predicted f_{obs}**	**Status**	**Interpretation**
Vacuum (~ 10 TeV)	**160 GHz**	**Observed**	**CMB [15]**
BSM Particle (~ 1.3 TeV)	3 GHz	Observed	ARCADE 2 Excess [16]
Higgs (125 GeV)	**24.6 MHz**	**Predicted**	**The "Higgs Horizon" (Hidden)**
Proton (0.938 GeV)	1.4 kHz	Coincidence	VLF Band Background [20]

Table 2: The RHM Kinematic Horizon Spectrum. The 10 TeV vacuum scale is inferred from the CMB peak [15]; other values are derived scalings.

7.5.3 The Higgs Horizon Feature

A specific, falsifiable prediction of the RHM is the existence of a non-thermal spectral excess centered at $\nu \approx 24.6$ MHz. In our framework, the Higgs mass ($m_H \approx 125$ GeV [6]) sets the tension scale for the vacuum expectation value.

We refer to this predicted signal as the **Higgs Horizon Feature**. This feature arises not from the decay of Higgs bosons, but from the horizon saturation of the Higgs-scale vacuum tension, which is reprocessed into the electromagnetic background via the mechanism described above.

Detection of this signal faces significant hurdles due to the Earth's ionospheric cutoff (~ 10 MHz). Consequently, the RHM predicts that the upcoming LuSEE-Night mission (scheduled for lunar farside deployment in late 2025/early 2026, sensitive to 0.1–50 MHz) and future lunar farside radio arrays (e.g., proposed FARSIDE concepts) will detect a distinct background excess centered at ≈ 25 MHz that is currently invisible to ground-based astronomy.

7.5.4 Interpretation of the ARCADE 2 Excess

The ARCADE 2 experiment reports an apparent excess in the extragalactic radio background over the $3 - 90$ GHz range, often modeled as a power-law component beyond standard source counts [16, 17].

In the RHM framework, we associate the lower end of this excess (3 GHz) with a characteristic horizon saturation mass of $m \approx 1.3$ TeV. This suggests that the ARCADE 2 excess could encode the kinematic horizon signature of **TeV-scale physics** (e.g., Supersymmetry or Composite sectors), populating the spectral band between the predicted Higgs horizon (25 MHz) and the fundamental Vacuum Tension (160 GHz).

7.5.5 Caveats and Observational Tests

We distinguish between the robust predictions of the model and phenomenological coincidences.

- **The CMB Anchor:** The association of the 160 GHz CMB peak with a 10 TeV vacuum scale is a derived inference; the model requires this scale to exist for the vacuum to be stable.
- **The Proton-VLF Coincidence:** While the proton mass maps to ~ 1.4 kHz, this band is dominated by terrestrial atmospheric noise (whistlers) [20]. We do not claim current VLF observations constitute detection of a proton horizon, but we predict a residual isotropic component in this band.
- **The Falsification Test:** The most direct test of the RHM is the 25 MHz band. If LuSEE-Night or future lunar-based arrays achieve sufficient sensitivity and find a purely thermal background with no excess at the Higgs frequency, the kinematic horizon hypothesis in its current form would be falsified.

8 Conclusion: A Falsifiable Geometric Framework

The Relational Harmonics Model proposes a shift from treating quantum numbers as abstract labels to treating them as consequences of harmonic phase geometry on layered internal degrees of freedom. While this work does not yet reproduce the full dynamical machinery of Quantum Field Theory, it provides a geometric organizing framework together with concrete phenomenological proposals:

1. **Proposed Higgs Horizon Feature:** A non-thermal spectral excess potentially centered at $\nu \approx 24.6$ MHz, arising from the proposed horizon saturation of the Higgs scale tension. This feature should be testable with upcoming missions such as LuSEE-Night (expected lunar farside deployment and data in 2026, sensitive to 0.1–50 MHz) or future low-frequency lunar arrays.

2. **TeV-Scale Radio Excess Interpretation:** The ARCADE-2 excess as a possible broadband kinematic horizon signature of $\mathcal{O}(1)$–10 TeV physics, bridging the proposed Higgs horizon and the ~ 10 TeV vacuum-tension scale associated with the CMB peak at ~ 160 GHz.

By grounding Standard Model parameters in a testable harmonic ontology, the RHM offers a pathway toward geometric unification of internal quantum numbers, horizon kinematics, and background spectra. Non-detection of the proposed 24.6 MHz excess upon sufficient observational sensitivity would falsify the specific kinematic horizon mechanism presented here, prompting refinements (e.g., modified saturation or emission coupling) while preserving the model's core structural representations of charges and color.

References

[1] Aad, G. *et al.* (ATLAS Collaboration). Observation of a new particle in the search for the Standard Model Higgs boson with the ATLAS detector at the LHC. *Phys. Lett. B* **716**, 1–29 (2012).

[2] Gell-Mann, M. A schematic model of baryons and mesons. *Phys. Lett.* **8**, 214–215 (1964).

[3] Ginzburg, V. L. & Landau, L. D. On the theory of superconductivity. *Zh. Eksp. Teor. Fiz.* **20**, 1064 (1950).

[4] Aker, M. *et al.* (KATRIN Collaboration). Direct neutrino-mass measurement with sub-electronvolt sensitivity. *Nature Phys.* **18**, 160–166 (2022).

[5] Aghanim, N. *et al.* (Planck Collaboration). Planck 2018 results. VI. Cosmological parameters. *Astron. Astrophys.* **641**, A6 (2020).

[6] Workman, R. L. *et al.* (Particle Data Group). Review of Particle Physics. *Prog. Theor. Exp. Phys.* **2022**, 083C01 (2022).

[7] Wilson, K. G. Confinement of quarks. *Phys. Rev. D* **10**, 2445–2459 (1974).

[8] Peskin, M. E. & Schroeder, D. V. *An Introduction to Quantum Field Theory.* (Addison-Wesley, Reading, USA, 1995).

[9] Poincaré, H. Sur la dynamique de l'électron. *Rend. Circ. Mat. Palermo* **21**, 129–175 (1906).

[10] Weinberg, S. *The Quantum Theory of Fields, Vol. 1: Foundations.* (Cambridge Univ. Press, Cambridge, UK, 1995).

[11] Gross, D. J. & Wilczek, F. Ultraviolet behavior of non-abelian gauge theories. *Phys. Rev. Lett.* **30**, 1343–1346 (1973).

[12] Chatrchyan, S. *et al.* (CMS Collaboration). Observation of a new boson at a mass of 125 GeV with the CMS experiment at the LHC. *Phys. Lett. B* **716**, 30–61 (2012).

[13] Fukuda, Y. *et al.* (Super-Kamiokande Collaboration). Evidence for oscillation of atmospheric neutrinos. *Phys. Rev. Lett.* **81**, 1562–1567 (1998).

[14] Sakharov, A. D. Vacuum quantum fluctuations in curved space and the theory of gravitation. *Sov. Phys. Dokl.* **12**, 1040–1041 (1968).

[15] Fixsen, D. J. *et al.* The cosmic microwave background spectrum from the full COBE FIRAS data set. *Astrophys. J.* **473**, 576 (1996).

[16] Fixsen, D. J. *et al.* ARCADE 2 measurement of the absolute sky brightness at 3-90 GHz. *Astrophys. J.* **734**, 5 (2011).

[17] Seiffert, M. *et al.* Interpretation of the ARCADE 2 absolute sky brightness measurement. *Astrophys. J.* **734**, 6 (2011).

[18] Burns, J. O. *et al.* Global 21-cm cosmology from the farside of the Moon. *Phil. Trans. R. Soc. A* **379**, 20190564 (2021).

[19] Burns, J. O. *et al.* Dark Ages Polarimeter Pathfinder 'DAPPER': A SMEX Mission Concept. *LPI Contributions* **2152**, 5035 (2019).

[20] Helliwell, R. A. *Whistlers and Related Ionospheric Phenomena.* (Stanford University Press, 1965).